

LLCL-Filter Based Single-Phase Grid-Tied Aalborg Inverter

Wu, Weimin; Feng, Shuangshuang; Ji, Junhao; Huang, Min; Blaabjerg, Frede

Published in:

Proceedings of the 2014 International Power Electronics and Application Conference and Exposition (PEAC2014)

DOI (link to publication from Publisher):

[10.1109/PEAC.2014.7037935](https://doi.org/10.1109/PEAC.2014.7037935)

Publication date:

2014

Document Version

Early version, also known as pre-print

[Link to publication from Aalborg University](#)

Citation for published version (APA):

Wu, W., Feng, S., Ji, J., Huang, M., & Blaabjerg, F. (2014). LLCL-Filter Based Single-Phase Grid-Tied Aalborg Inverter. In *Proceedings of the 2014 International Power Electronics and Application Conference and Exposition (PEAC2014)* (pp. 658-663). IEEE Press. <https://doi.org/10.1109/PEAC.2014.7037935>

General rights

Copyright and moral rights for the publications made accessible in the public portal are retained by the authors and/or other copyright owners and it is a condition of accessing publications that users recognise and abide by the legal requirements associated with these rights.

- Users may download and print one copy of any publication from the public portal for the purpose of private study or research.
- You may not further distribute the material or use it for any profit-making activity or commercial gain
- You may freely distribute the URL identifying the publication in the public portal -

Take down policy

If you believe that this document breaches copyright please contact us at vbn@aub.aau.dk providing details, and we will remove access to the work immediately and investigate your claim.

LLCL-Filter Based Single-Phase Grid-Tied Aalborg Inverter

Weimin Wu, Shuangshuang Feng, Junhao Ji

Dept. of Electrical Engineering
Shanghai Maritime University
Shanghai, China
wmwu@shmtu.edu.cn

Min Huang, Frede Blaabjerg

Dept. of Energy Technology
Aalborg University
Aalborg, Denmark
fbl@et.aau.dk

Abstract—The Aalborg Inverter is a new type of high efficient DC/AC grid-tied inverter, where the input DC voltage can vary in a wide range. Compared with the *LCL*-filter, the *LLCL*-filter can save the total inductance for the conventional voltage source inverter. In this paper, an *LLCL*-filter based Aalborg Inverter is proposed and its character is illustrated through the small signal analysis in both “Buck” and “Buck-Boost” mode. From the modeling, it can be seen that the resonant inductor in the capacitor loop has not brought extra control difficulties, whereas more inductance in the power loop can be saved. Simulation and experiments are carried out to verify the analysis and the design through an 220 V/50 Hz, 2000 W prototype.

Keywords—Grid-tied Inverter; *LLCL*-filter; *VSI*; Modelling;

I. INTRODUCTION

With the development of renewable energy generation, grid-connected inverters are being more and more widely used [1]-[9]. In order to achieve higher efficiency for photovoltaic (PV) inverter, recently, the MOSFET switch based inverters are becoming popular [5]-[9]. The Aalborg Inverter is a new family of high efficiency MOSFET switch based transformerless inverter operating with a wide variation of input DC voltage, which working states depend on the instantaneous difference between the input voltage and the output voltage [9],[10]. Similar to the conventional dual mode time-sharing inverters [11]-[12], it has minimum switching power loss since only one power stage of this inverter chops at high frequency at any time. Furthermore, a voltage drop on the filtering inductor in the power loop can be decreased with the reduced size and power losses [10].

In the application, the output filter also affects the efficiency of grid-tied inverter [13]. In order to save the total inductance of a voltage source grid-tied inverter and increase the system efficiency, the *LLCL*-filter was proposed in [14], where nearly zero impedance at the switching frequency can be achieved, strongly attenuating the harmonic currents around the switching frequency. Comparing to the *LCL*-filter, the *LLCL*-filter has not brought extra control difficulty for a grid-tied inverter [14]-[17]. The EMI issue caused by the resonant inductor in the capacitor loop of the *LLCL*-filter can easily be solved at smaller cost [18]-[20].

It can be deduced that when the *LLCL*-filter is applied in the Aalborg inverter, the efficiency of whole system can be further improved. This paper focuses on the small signal

modeling of the *LLCL*-filter based Aalborg Inverter. The main circuit and basic operating principle is first introduced. Then, the modeling of this inverter is carried out during “Buck” and “Boost” operation state. Finally, simulations and experiments are carried out on a 2 kW prototype in order to verify the theoretical analysis.

II. THE MAIN CIRCUIT AND THE BASIC OPERATING PRINCIPLE OF *LLCL*-FILTER BASED AALBORG INVERTER

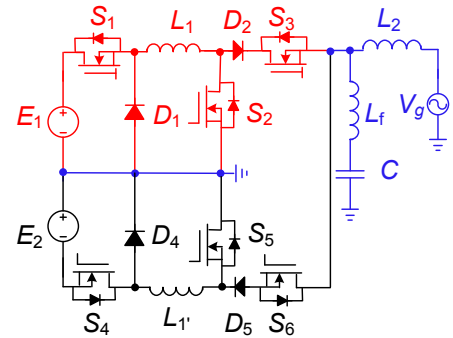


Fig. 1. Circuit diagram of the proposed *LLCL*-filter based Aalborg Inverter.

Fig. 1 shows the proposed *LLCL*-filter based single-phase grid-tied Aalborg Inverter, where an inductor L_f is in series with C , composing a resonant circuit at the switching frequency (note that the switching frequency of S_1 , S_2 , S_4 and S_5 is set to be the same value of $1/T_s$) to attenuate the switching frequency harmonics of the grid-injected current. The main circuit is vertically symmetrical except for the components of L_f , C and L_2 . During the positive period of the grid voltage, the upper part (in red) works, while the lower part (in black) does not operate. During the negative period, they work inversely. In this paper, only the positive period is analyzed.

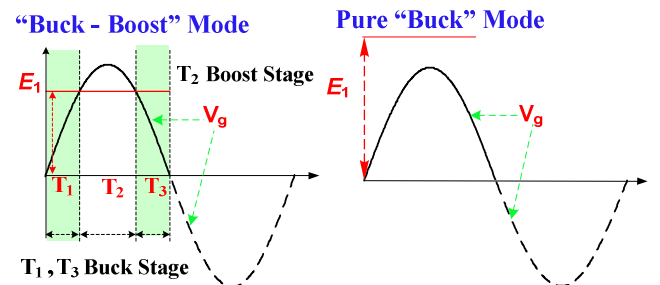


Fig. 2. Operating principle of the proposed *LLCL*-filter based Aalborg Inverter.

This work was partially supported by the Innovation Project of Shanghai Municipal Education Commission under Award 13ZZ125, the Project of Shanghai Natural Science Foundation under Award 12ZR1412400, and the Project of Shanghai PuJiang Program under Award 14PJ1404200.

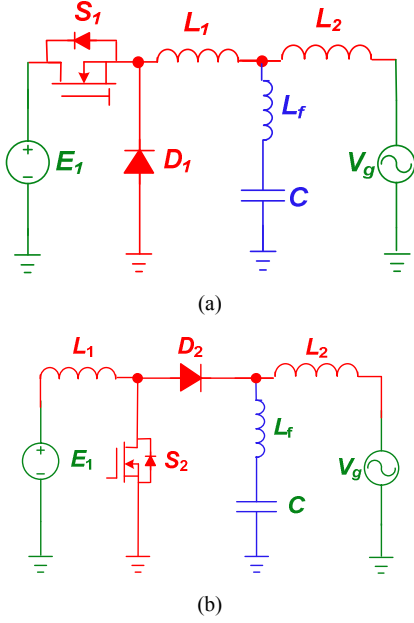


Fig. 3. Equivalent circuits of LLCL-filter based Aalborg Inverter: (a) Buck stage, (b) Boost stage.

As shown in Fig. 2, there are two different working modes for this inverter. When the instantaneous value of the grid voltage is lower than the input DC voltage (in the pure “Buck” mode or during T_1 , T_3 of the “Buck-boost” mode), the Aalborg Inverter operates in the “Buck” stage, where the equivalent circuit is shown in Fig. 3 (a). Also, when the input DC voltage is lower than the instantaneous value of the grid voltage, as shown during T_2 of the “Buck-boost” mode in Fig. 2, the inverter works in the “Boost” stage, and the equivalent circuit can be drawn in Fig. 3 (b).

Like the conventional dual-mode time-sharing inverters [8], [11], [12], [21], only one power stage of this inverter operates at high frequency at any time. The switching power losses can be reduced a lot, compared to the traditional two-stage voltage source inverter with a DC / DC boost converter.

III. MODELING OF THE LLCL FILTER BASED AALBORG INVERTER

A. During the “Buck” Stage

In this section, the small signal modelling on this inverter will be carried out. It should be pointed that the small signal model only fits for the constant output in theory, but the grid voltage can also be treated as being in the “steady state,” since it is changing with the line frequency only, which is much lower than the high switching frequency [21],[22].

During the “Buck” stage, the inverter is simplified as shown in Fig. 3 (a), and the equivalent circuit in one duty cycle is illustrated in Fig. 4.

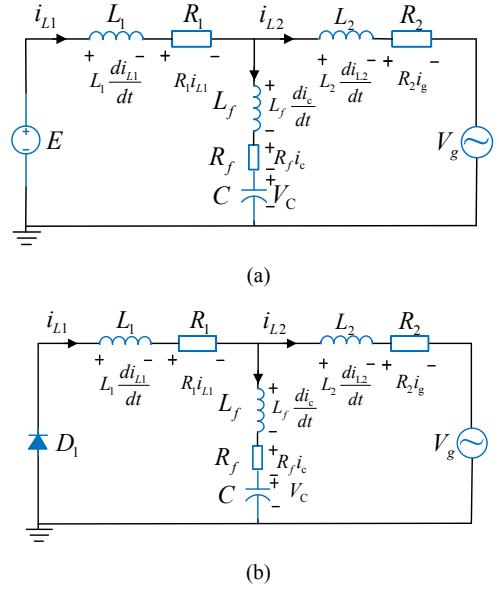


Fig. 4. Equivalent small signal circuits during the “Buck” stage (a) $[t, t + dT_s]$, (b) $[t + dT_s, t + T_s]$.

Unlike DC / DC converters, DC / AC inverter does not have a steady state during the line frequency period, but it could be treated as a quasi-steady-state in a switching period, while analyzing one steady state working point, where the quasi-steady state equation can be given as,

$$\begin{cases} V_c = E \cdot D - I_{L1} \cdot R_1 \\ I_{L1} = I_{L2} \\ V_c = I_{L2} \cdot R_2 + V_g \end{cases} \quad (1),$$

where D is the duty cycle of the Buck switch S_1 , I_{L1} and I_{L2} are the average currents of L_1 and L_2 in a duty cycle, E (E_1 or E_2) is half of the input DC voltage, R_1 and R_2 are the equivalent resistors of inductor L_1 and L_2 , respectively.

Using the steady state equation and ignoring the high-order terms, the linear small signal AC model of the system during the “Buck Stage” can be derived as,

$$\begin{cases} L_1 \frac{d\hat{i}_{L1}(t)}{dt} = E_1 \cdot \hat{d}(t) + D \cdot \hat{e}(t) - \hat{i}_{L1}(t) \cdot R_1 - \hat{v}_c(t) \\ C \frac{d\hat{v}_c(t)}{dt} = \hat{i}_{L1}(t) - \hat{i}_{L2}(t) \\ L_2 \frac{d\hat{i}_{L2}(t)}{dt} = \hat{v}_c(t) - \hat{i}_{L2}(t) \cdot R_2 - \hat{v}_g(t) \end{cases} \quad (2).$$

where $\hat{x}(t)$ is the small ac variation of X .

Assuming the input voltage perturbation of $\hat{e}(t) = 0$ and the grid voltage perturbation of $\hat{v}_g(t) = 0$ and doing Laplace transformation to (2), then the transfer function of the grid-injected current versus the control can be obtained as,

$$G_{buck}(s) = \left. \frac{\hat{i}_{L2}(s)}{\hat{d}(s)} \right|_{\substack{\hat{e}(s)=0 \\ \hat{v}_g(s)=0}} = \frac{E}{L_1 L_2 C s^3 + (L_1 C R_2 + L_2 C R_1) s^2 + (L_2 + R_1 R_2 C + L_1) s + R_2 + R_1} \quad (3),$$

B. During the “Boost” Stage

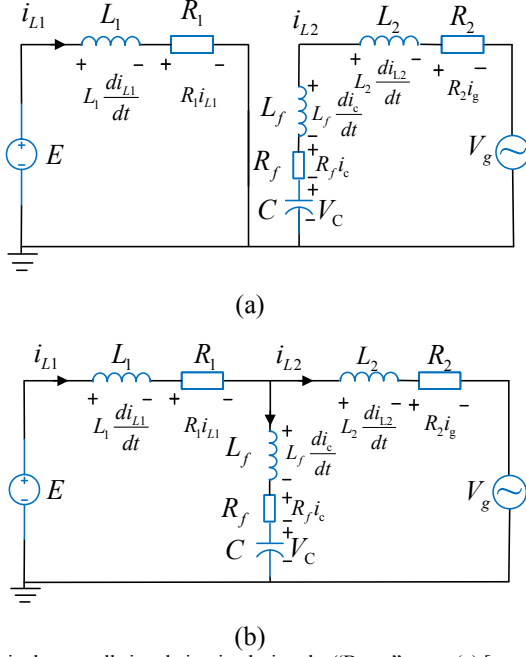


Fig. 5. Equivalent small signal circuits during the “Boost” stage (a) $[t, t + dT_s]$, (b) $[t + dT_s, t + T_s]$.

$$G_{boost}(s) = \frac{\hat{i}_{L1}(s)}{\hat{d}'(s)} \bigg|_{\substack{\hat{V}_{in}(s)=0 \\ \hat{e}_s(s)=0}} = \frac{V_{C1}L_2C_1s^2 + (V_{C1}C_1R_2 + (1-D')I_{L1}L_2)s + V_{C1} + (1-D')I_{L1}R_2}{s^3L_1L_2C_1 + s^2(L_2C_1R_1 + L_1C_1R_2) + s(C_1R_1R_2 + L_2(1-D')^2 + L_1) + R_1 + (1-D')^2R_2} \quad (6).$$

where D' is the duty cycle of the Boost switch S_2 .

C. Analysis on the Open Loop Gain

From (3), it can be seen that during the “Buck” stage, the controller design has no relation with the duty cycle. However, equation (6) shows that the bode diagram varied with the duty cycle during the “Boost” stage. Since the largest boost ratio takes place at the time of appearance of the AC voltage peak value, in theory, the worst control case also appears at this moment.

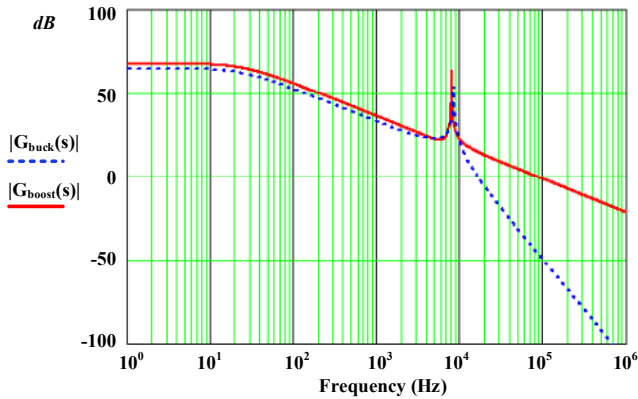


Fig. 6. Gain diagram of the control to output current transfer function.

During the “Boost” stage, the inverter can be simplified as shown in Fig. 3 (b). The equivalent circuit in one duty cycle is illustrated in Fig. 5. In this paper, the indirect current control method [22] is adopted, where the system is assumed as an ideal system without any power losses and the instantaneous input power equals to the instantaneous output power, which can be described as,

$$E(t) \cdot i_1(t) = V_g(t) \cdot i_{L2}(t) \quad (4)$$

Then, the given current of the Boost inductor can be derived as

$$i_{ref_L1}(t) = \frac{|V_g(t)|^2}{R_E \cdot E} \quad (5),$$

where R_E is the equivalent resistor for calculating the generated power.

Similar to the modelling method using for the “Buck” stage, the control to the DC current of Boost inductor $i_{L1}(t)$ transfer function can be derived as the following,

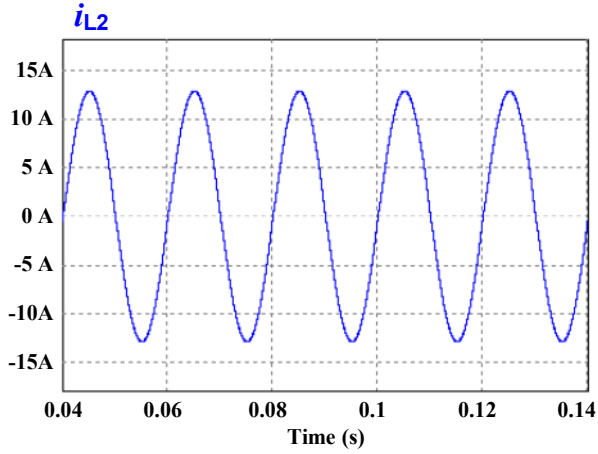
TABLE I. Main parameters of the LCL filter and the LLCL filter.

Filter	L_1, L_V (mH)	R_1 (Ω)	L_2 (mH)	R_2 (Ω)	L_f (μ H)
LCL	0.6	0.1	0.6	0.1	-
LLCL	0.6	0.1	0.25	0.02	8
Filter	R_f (Ω)	C (μ F)	V_g (V)	E_1, E_2 (V)	I_g (A)
LCL	-	2	220	350/240	12.8(peak)
LLCL	0.01	2	220	350/240	12.8(peak)

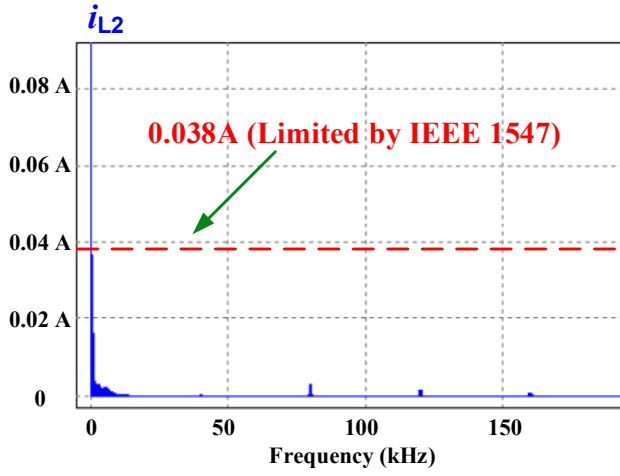
Fig. 6 shows the gain diagrams of the control to the current transfer function, where the parameters are listed in Table I. Note that the gain of $G_{boost}(s)$ is in the worst case. It can be also seen that within the characteristic frequency, the gain diagrams of the two stages are very similar. Then it can be deduced that the controller structure could be the same both in “Boost” and “Buck” stages, making it easy to design the controller.

IV. SIMULATIONS AND EXPERIMENTAL RESULTS

Based on the modeling, simulations are carried out, where conventional PI controller is adopted for the control. The designed parameters are also listed in Table I. The switching frequency of S_1, S_2, S_4 and S_5 is 40 kHz, and the S_3 and S_6 works in every half of the line period.

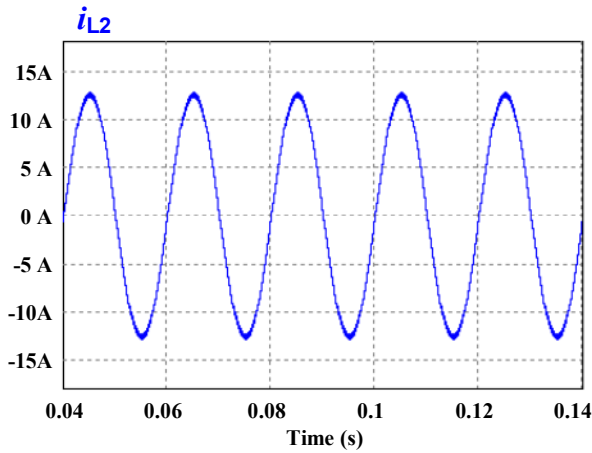


(a)

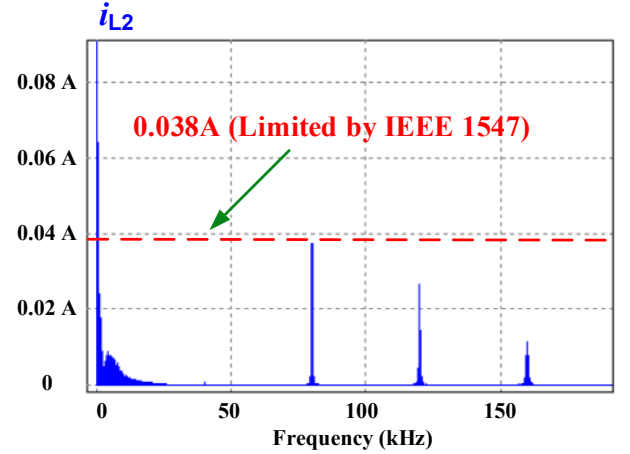


(b)

Fig. 7. Simulated grid-injected current in the pure “Buck” Mode ($E_1 = E_2 = 350$ V) (a) Grid-injected current, (b) Spectrum.



(a)



(b)

Fig. 8. Simulated grid-injected current in the “Buck-Boost” Mode ($E_1 = E_2 = 240$ V) (a) Grid-injected current, (b) Spectrum.

Fig. 7 shows the grid-injected current of the *LLCL*-filter based Aalborg inverter, which works in pure “Buck” mode, where the input DC voltage is 700 V and the output AC voltage is 220 V / 50 Hz. The amplitude of the dominant harmonic current is below the limitation of $0.3\% \cdot 12.8 = 0.038$ A, as specified by IEEE-1547.2-2008 [23].

Fig. 8 shows the grid-injected current in the “Buck-Boost” mode, where the input DC voltage is 480 V. It can be seen that the amplitude of the dominant harmonic current is close to the limitation of 0.038 A, maybe due to the higher current ripple caused by the “Boost” stage operation.



Fig. 9. Photo of the experimental Setup.

An 220V/50Hz/2000 W *LLCL*-filter based Aalborg inverter prototype based on a DSP (TMS320LF2812) controller is designed and constructed. The type of MOSFETs is IPW60R045CP, and the type of diodes is IDW30G65C5. Two DC power supplies (Chroma 62120) provide the DC power and a programmable AC source (Chroma 6530) is used to emulate the grid voltage. The parameters are the same as those in the simulations. Fig. 9

shows picture of the experimental prototype. During the experiments, the parameters are the same as those for simulations.

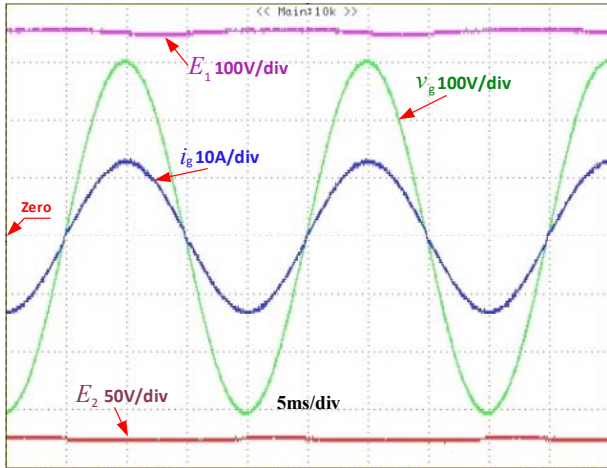


Fig. 10. Measured input DC voltages (E_1 , E_2), grid voltage (V_g) and grid-injected current (i_g) in the “Buck” Mode ($E_1 = E_2 = 350$ V).

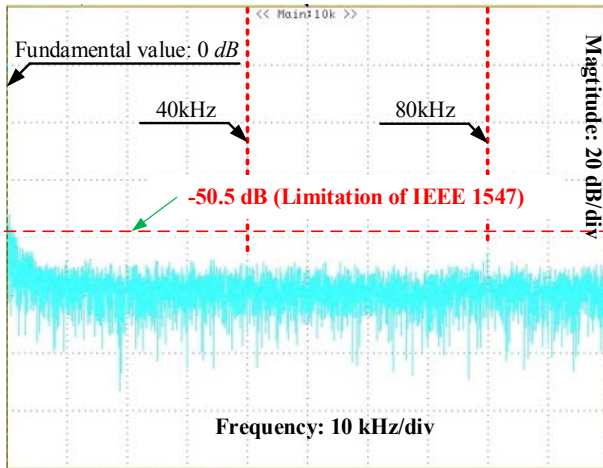


Fig. 11. Power spectrum of grid-injected current in the “Buck” Mode ($E_1 = E_2 = 350$ V).

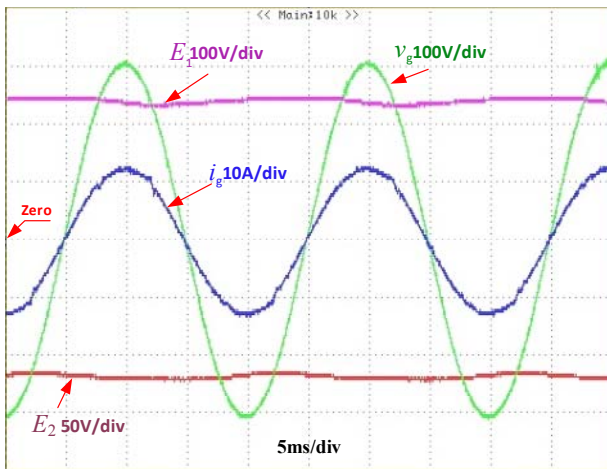


Fig. 12. Measured input DC voltages (E_1 , E_2), grid voltage (V_g) and grid-injected current (i_g) in the “Buck-Boost” Mode ($E_1 = E_2 = 240$ V).

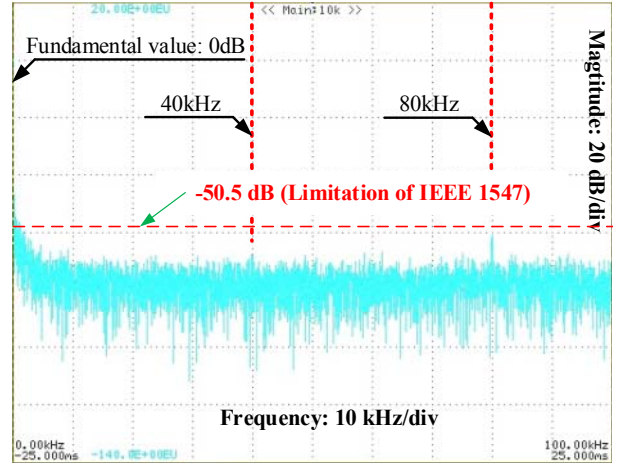


Fig. 13. Power spectrum of grid-injected current in the “Buck-Boost” Mode ($E_1 = E_2 = 240$ V).

When the input DC voltage is 700 V, the measured input DC voltages (E_1 , E_2), grid voltage (V_g), and grid-injected current (i_g) are shown in Fig. 10, and the power spectrum of the grid-injected current is shown in Fig. 11. Fig. 12 shows the grid-injected current, the grid voltage and the input DC voltage in the “Buck” mode ($E_1 = E_2 = 240$ V), while the spectrum of the grid-injected current is shown in Fig. 13. Comparing Figs. 10- 13 with Figs. 7-8, it can be seen that the experiments match the simulation results very well.

V. CONCLUSION

In this paper, the *LLCL*-filter based single-phase grid-tied Aalborg Inverter is proposed. The small signal modeling is carried out in details. From the modeling, it can be seen that compared with the *LCL*-filter based Aalborg inverter[7], the *LLCL*-filter based one has not brought the extra control difficulties either in the “Buck” mode or in the “Buck-Boost” mode, whereas the more inductance in the power loop has been saved. Simulations and experiments have been carried out to confirm the theoretical analysis through a 220 V / 50 Hz, 2000 W prototype.

REFERENCES

- [1] J. W. Kolar, T. Friedli, J. Rodriguez, and P. W. Wheeler, “Review of Three-Phase PWM AC–AC Converter Topologies”, *IEEE Trans. on Ind. Electron.*, vol. 58, no. 11, pp. 4988–5006, Nov. 2011.
- [2] D. Meneses, F. Blaabjerg, Ó. García, J. A. Cobos, “Review and Comparison of Step-up Transformerless Topologies for Photovoltaic AC-Module Application”, *IEEE Trans. on Power Electron.*, vol. 28, no. 6, pp. 2649–2663, June 2013.
- [3] F. Blaabjerg, M. Liserre, K. Ma, “Power Electronics Converters for Wind Turbine Systems”, *IEEE Trans. on Ind. Applicat.*, vol. 48, no. 2, pp. 708–719, March/April 2012.
- [4] S.B. Kjaer, J.K. Pedersen, F. Blaabjerg, “A review of single-phase grid-connected inverters for photovoltaic modules”, *IEEE Trans. on Ind. Applicat.*, vol. 41, no. 5, pp. 1292–1306, Sept./Oct. 2005.
- [5] P. Sun, C. Liu, J.-S. Lai, C.-L. Chen, “Cascade Dual Buck Inverter With Phase-Shift Control,” *IEEE Trans. on Power Electron.*, vol. 27, no. 4, pp. 2067–2077, April 2012.

- [6] Z. Yao, L. Xiao, "Two-Switch Dual-Buck Grid-Connected Inverter With Hysteresis Current Control," *IEEE Trans. on Power Electron.*, vol. 27, no. 7, pp. 3310-3318, July 2012
- [7] Z. Zhao, M. Xu, Q. Chen, J. Lai, and Y. Cho, "Derivation, Analysis, and Implementation of a Boost-Buck Converter-Based High-Efficiency PV Inverter," *IEEE Trans. on Power Electron.*, vol. 27, no. 3, pp. 1304 – 1313, March 2012.
- [8] B. Chen, B. Gu, L. Zhang, Z.U. Zahid, Jih-Sheng Lai, Z. Liao, R. Hao, "A High Efficiency MOSFET Transformerless Inverter for Non-isolated Micro-inverter Applications", *IEEE Trans. on Power Electron.*, in press, 2014.
- [9] W. Wu and F. Blaabjerg, "Aalborg Inverter-A new type of "Buck in Buck, Boost in Boost" Grid-tied Inverter ", *In Proc. of APEC2013*, CA, Mach 17-21, 2013, pp. 460-467.
- [10] W. Wu, Z. Wang, J. Ji, F. Blaabjerg, "Performance Analysis of New Type Grid-tied Inverter-Aalborg Inverter" *In Proc. of ECCE (Europe)2014*, Lappeenranta, Finland, Aug. 26-28, 2014.
- [11] K. Ogura, T. Nishida, E. Hiraki, M. Nakaoka, S. Nagai, "Time-sharing boost chopper cascaded dual mode single-phase sinewave inverter for solar photovoltaic power generation system", *In Proc. of PESC'04*, Aachen, Germany, June 20-25, 2004, pp. 4763 – 4767.
- [12] W. Wu, and T. Tang, "Dual Mode Time-Sharing Cascaded Sinusoidal Inverter", *IEEE Trans. on Energy Conv.*, vol. 22, no. 3, pp. 795-797, Sept. 2007.
- [13] W. Wu, M. Huang, F. Blaabjerg, "Efficiency comparison between the *LLCL* and *LCL*-filters based single-phase grid-tied inverters." *Archives of Electrical Engineering*, vol. 63, no. 1, pp. 63-79, March 2014.
- [14] W. Wu, Y. He, and F. Blaabjerg, "An *LLCL*- Power Filter for Single-phase Grid-tied Inverter", *IEEE Trans. on Power Electron.*, vol. 27, no. 2, pp. 782-789, Feb. 2012.
- [15] W. Wu, Y. He, T. Tang, and F. Blaabjerg, "A New Design Method for the Passive Damped *LCL*- and *LLCL*-Filter Based Single-Phase Grid-tied Inverter", *IEEE Trans. on Ind. Electron.*, vol. 60, no. 10, pp. 4339-4350, Oct. 2013.
- [16] W. Wu, Z. Lin, Y. Sun, X. Wang, M. Huang, H. Wang, Chung, H. S. H, "A hybrid damping method for *LLCL*-filter based grid-tied inverter with a digital filter and an RC parallel passive damper", *In Proc. of ECCE 2013*, Colorado USA, Sept. 15-19, 2013, pp. 456 - 463.
- [17] W. Wu, Y. Sun, M. Huang, X. Wang, H. Wang, Blaabjerg, F, Chung, H. S. H, "A Robust Passive Damping Method for *LLCL*-Filter Based Grid-Tied Inverters to Minimize the Effect of Grid Harmonic Voltages", *IEEE Trans. on Power Electron.*, vol. 29, no. 7, pp. 3279-3289, July. 2014.
- [18] W. Wu, Y. Sun, Z. Lin, Y. He, M. Huang, Blaabjerg, F, Chung, H. S. H., "A Modified *LLCL*-Filter With the Reduced Conducted EMI Noise," *IEEE Trans. on Power Electron.*, vol. 29, no. 7, pp. 3393-3402, July 2014.
- [19] J. Xu, J. Yang, J. Ye, Z. Zhang, A. Shen, "An *LTCL* Filter for Three-Phase Grid-Connected Converters", *IEEE Trans. on Power Electron.*, in press, 2014.
- [20] W. Wu, Y. Sun, Z. Lin, T. Tang, Blaabjerg, F, Chung, H. S. H, "A New *LCL*-filter with In-Series parallel Resonant Circuit for Single-phase Grid-tied inverter", *IEEE Trans. on Ind. Electron.*, pp. 4640 – 4644, Sept. 2014.
- [21] Z. Zhao, J. Lai, Y. Cho, "Dual-Mode Double-Carrier-Based Sinusoidal Pulse Width Modulation Inverter With Adaptive Smooth Transition Control Between Modes", *IEEE Trans. on Ind. Electron.*, vol. 60, no. 5, pp. 2094 – 2103, May 2013.
- [22] W. Wu, H. Geng, P. Geng, Y. Ye, and M. Chen, "A Novel Control Method for Dual Mode Time-sharing Grid-connected Inverter", *In Proc. of ECCE 2010*, pp. 53-57, Atlanta, GA, USA, Sept. 12-16, 2010.
- [23] "IEEE Standard for Interconnecting Distributed Resources with Electric Power Systems", *IEEE 1547.2-2008*, 2008.